Developmental Cell
Article

CBP Histone Acetyltransferase Activity Regulates Embryonic Neural Differentiation in the Normal and Rubinstein-Taybi Syndrome Brain

Jing Wang,[1,2] Ian C.G. Weaver,[1,2] Andrée Gauthier-Fisher,[1,2] Haoran Wang,[5] Ling He,[6] John Yeomans,[5] Frederic Wondisford,[6] David R. Kaplan,[2,3] and Freda D. Miller[1,3,4,*]
[1]Developmental and Stem Cell Biology Program
[2]Cell Biology Program
Hospital for Sick Children, 555 University Ave., Toronto, ON, Canada M5G 1X8
[3]Department of Molecular Genetics
[4]Department of Physiology
[5]Department of Psychology
Medical Sciences Building, University of Toronto, Toronto, ON, Canada M5S 1A8
[6]Department of Pediatrics and Medicine, Johns Hopkins Medical School, Baltimore, MD 21287, USA
*Correspondence: fredam@sickkids.ca
DOI 10.1016/j.devcel.2009.10.023

SUMMARY

Increasing evidence indicates that epigenetic changes regulate cell genesis. Here, we ask about neural precursors, focusing on CREB binding protein (CBP), a histone acetyltransferase that, when haploinsufficient, causes Rubinstein-Taybi syndrome (RTS), a genetic disorder with cognitive dysfunction. We show that neonatal *cbp*$^{+/-}$ mice are behaviorally impaired, displaying perturbed vocalization behavior. *cbp* haploinsufficiency or genetic knockdown with siRNAs inhibited differentiation of embryonic cortical precursors into all three neural lineages, coincident with decreased CBP binding and histone acetylation at promoters of neuronal and glial genes. Inhibition of histone deacetylation rescued these deficits. Moreover, CBP phosphorylation by atypical protein kinase C ζ was necessary for histone acetylation at neural gene promoters and appropriate differentiation. These data support a model in which environmental cues regulate CBP activity and histone acetylation to control neural precursor competency to differentiate, and indicate that *cbp* haploinsufficiency disrupts this mechanism, thereby likely causing cognitive dysfunction in RTS.

INTRODUCTION

There is increasing interest in the idea that epigenetic changes regulate the behavior of somatic tissue stem cells (Lunyak and Rosenfeld, 2008). One epigenetic modification that directly regulates chromatin structure is histone acetylation, which is determined by two enzyme classes: the histone deacetylases (HDACs) (Haberland et al., 2009), and the histone acetyltransferases (HATs). Of the HATs, two of the best characterized are CREB binding protein (CBP) and its closely related family member, p300 (Chan and La Thangue, 2001). CBP is a transcriptional coactivator that interacts with over 300 transcription factors, and binds to components of the general transcriptional machinery (Chan and La Thangue, 2001). Intriguingly, CBP and p300 regulate hematopoietic stem cells (Rebel et al., 2002), raising the possibility that they might generally regulate stem cell biology.

Rubinstein-Taybi syndrome (RTS) is a genetic disorder with cognitive dysfunction, where one allele of CBP is deleted or mutated (Roelfsema and Peters, 2007). *cbp*$^{+/-}$ mice display cognitive dysfunction in adulthood: these perturbations are attributed to aberrant mature circuit function (Josselyn, 2005). However, cognitive deficits are evident in early childhood in RTS, and CBP interacts with developmentally important transcription factors (Miller and Gauthier-Fisher et al., 2007), suggesting that it might regulate embryonic neural development.

Here, we examine a potential role for CBP in developing neural precursors, focusing upon the cerebral cortex, which is generated from neuroepithelial stem cells that sequentially generate neurons, astrocytes, and oligodendrocytes (Miller and Gauthier, 2007). We provide evidence that phosphorylation of CBP by atypical protein kinase C (aPKC) ζ acts as an epigenetic switch to promote precursor differentiation, and that *cbp* haploinsufficiency perturbs this regulatory mechanism, thereby causing early cognitive dysfunction in mice as it does in humans.

RESULTS

cbp Haploinsufficiency Causes Early Cognitive Dysfunction in Mice as It Does in Humans

To determine whether *cbp*$^{+/-}$ mice display early cognitive dysfunction, we analyzed ultrasonic vocalizations (USVs) in neonatal mice; alterations in USVs reflect impaired cognition and social behavior (Branchi et al., 2001). Postnatal Day 10 (P10) mice were transiently isolated from their mothers and USVs recorded for 4 min immediately after separation. *cbp*$^{+/-}$ mice were significantly impaired relative to their wild-type littermates; USV numbers and duration were decreased, and USV peak frequencies increased (Figures 1A and 1B). Thus, neonatal *cbp*$^{+/-}$ mice are behaviorally impaired, indicating that CBP plays a role in neural development.

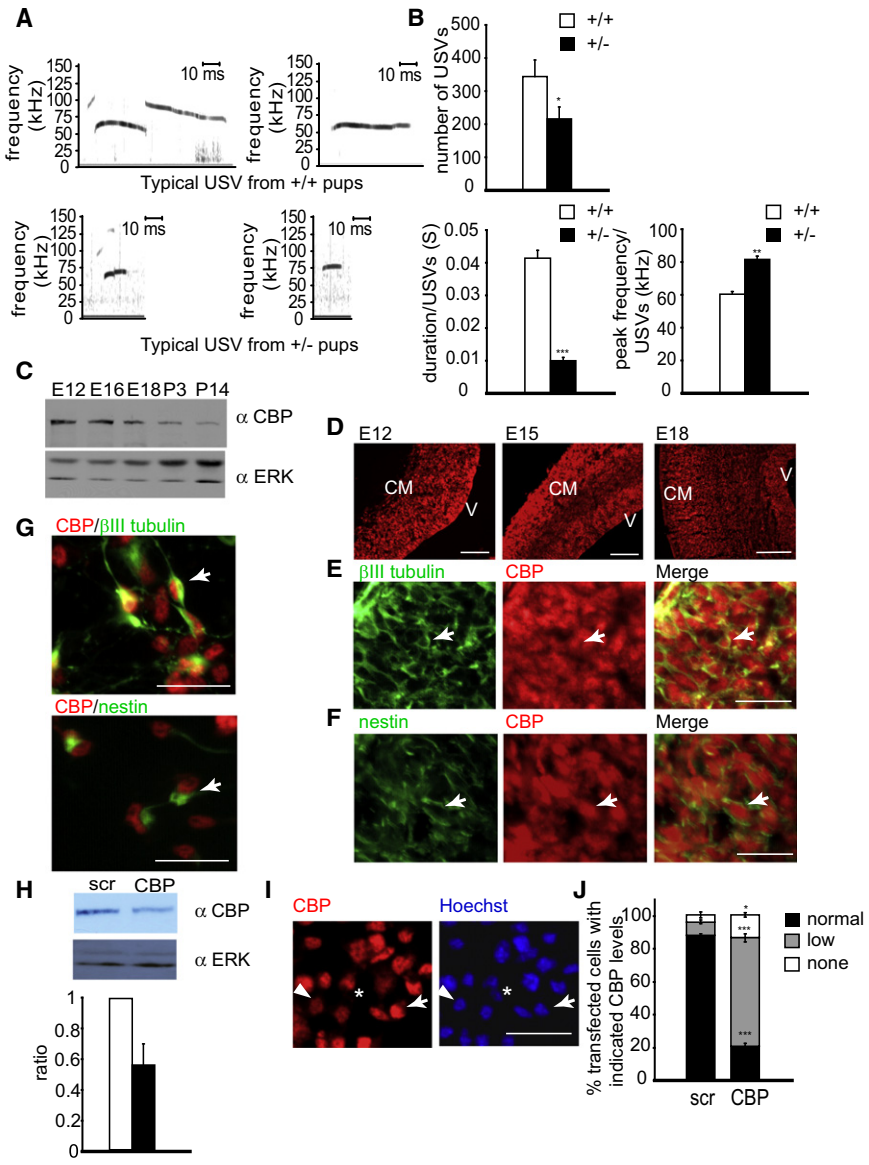

Figure 1. CBP Is Expressed in the Mouse Embryonic Cortex and Regulates Neurobehavioral Development

(A and B) *cbp* haploinsufficiency causes early behavioral deficits in USV. Representative USVs (A) and graphs (B) showing USV number, duration, and peak frequency (kHz) in $cbp^{+/-}$ versus $cbp^{+/+}$ P10 mice following maternal separation ($n \geq 7$ each).

(C–J) CBP is expressed in cortical precursors and newly-born cortical neurons. (C) Western blot for CBP in E12–P14 cortices. The blot was reprobed for ERK as a loading control. (D) Immunocytochemistry for CBP (red) in coronal sections of E12, E15, and E18 cortices showing expression in the VZ/SVZ next to the ventricle (v) and in the cortical mantle (CM). (E and F) Immunocytochemistry for CBP (red) and βIII-tubulin (E) or nestin (F) (both green) in the E15 cortical plate (E) or VZ/SVZ (F). Arrows denote double-labeled cells. (G) Immunocytochemistry for CBP (red) and βIII-tubulin (top) or nestin (bottom; both green) in 3 day precursor cultures. Arrows denote double-labeled cells. (H) Western blot for endogenous CBP in NIH 3T3 cells transfected with *cbp* or scrambled (scr) siRNAs, reprobed for ERK to ensure equal protein. The graph shows relative CBP levels determined by densitometry (n = 2). (I) CBP immunoreactivity (red) in cultured precursors. The arrow, arrowhead, and asterisk indicate cells with basal, low, and no detectable CBP, respectively. (J) Quantification of CBP levels as in (I) for precursors cotransfected with *egfp* and *cbp* or scrambled (scr) siRNAs for 5 days (n = 3 experiments, pooled).

*p < 0.05, **p < 0.01, ***p < 0.001. Scale bars, 100 ([D] left and middle), 250 ([D] right), or 25 μm (E–G and I). Error bars denote SEM.

CBP Regulates Cortical Precursor Differentiation, but Not Survival or Proliferation

To determine how CBP regulates neural development, we asked where it was expressed in the embryonic cortex. Western blots showed that CBP was expressed throughout embryogenesis, with levels decreasing postnatally (Figure 1C). Immunocytochemistry of cortical sections from E12 to E18 showed that CBP was expressed in both nestin-positive precursors of the VZ/SVZ and βIII-tubulin-positive neurons in the cortical mantle (Figures 1D–1F). To confirm these data, we immunostained primary E12–E13 cortical precursor cultures that sequentially generate neurons and glia (Barnabé-Heider et al., 2005; Gauthier-Fisher et al., 2007). As seen in vivo, CBP was present in the nuclei of nestin-positive precursors and βIII-tubulin-positive neurons (Figure 1G).

Based upon its expression, we sought to determine whether CBP regulated cortical precursor development by using siRNAs. To test the efficacy of *cbp* siRNAs, we transfected them into murine 3T3 cells and performed Western blots after 3 days; *cbp* siRNAs decreased endogenous CBP 2-fold, even though only 30%–50% of the cells were transfected (Figure 1H). We confirmed a similar knockdown in cortical precursors that were cotransfected with a nuclear EGFP plasmid. Nearly all precursors transfected with scrambled siRNAs expressed detectable CBP, while most precursors transfected with *cbp* siRNAs expressed low or no detectable CBP (Figures 1I and 1J).

Through the use of these siRNAs, we investigated whether CBP regulated cortical precursor development, examining survival and proliferation first. Immunostaining of transfected cells at 2 days showed that CBP knockdown had no effect on the percentage of cells expressing Ki67 or cleaved caspase-3, markers of proliferation and apoptosis, respectively (Figures 2A and 2B; see Figures S1A and S1B available online). CBP knockdown also had no effect on the percentage of transfected cells with condensed, apoptotic nuclei (Figure 2C). To determine whether CBP might instead regulate differentiation, we immunostained cultures for βIII-tubulin at 5 days; CBP knockdown caused a small but significant decrease in the number of neurons generated (Figures 2D

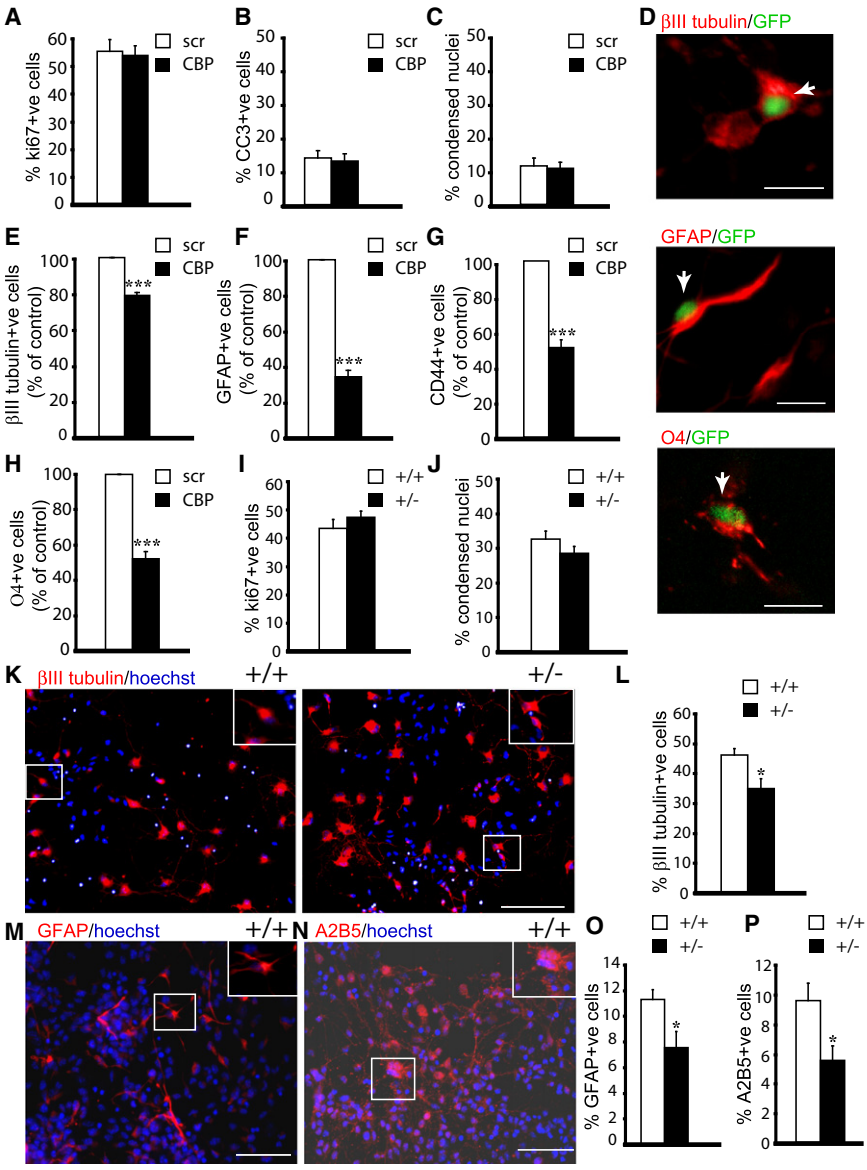

Figure 2. CBP Regulates Differentiation, but Does Not Affect Survival or Proliferation of Cortical Precursors

(A–C) Percentage of transfected, Ki67-positive cells (A), cleaved caspase-3 (CC3)-positive cells (B), or cells with condensed, apoptotic morphology (C) in precursors cotransfected with *egfp* and *cbp* or scrambled siRNAs for 2 days (n = 3 experiments each, pooled).

(D) Immunocytochemistry for EGFP (green) and βIII-tubulin (top), GFAP (middle), or O4 (bottom) (all red) in precursors cotransfected with *egfp* and scrambled siRNAs and cultured in basal conditions (top), or in CNTF (middle) or neuregulin β (bottom) for 5 days. Arrows indicate double-labeled cells.

(E–H) Relative percentage of transfected, βIII-tubulin-positive neurons (E), GFAP-positive or CD44-positive astrocytes (F and G), or O4-positive oligodendrocytes (H) in precursors transfected with *cbp* or scrambled siRNAs, as in (D) (n = 3 each, pooled).

(I and J) Percentage of cells that are Ki67 positive (I) or with apoptotic nuclei (J) in E12 $cbp^{+/+}$ versus $cbp^{+/-}$ precursors cultured for 2 days (n ≥ 6 single embryos each).

(K, M, and N) Immunocytochemistry (red) for βIII tubulin (K), GFAP (M), or A2B5 (N) in $cbp^{+/+}$ or $cbp^{+/-}$ precursors cultured for 3 days (K), or for 5 days in CNTF (M) or neuregulin β (N). Cells were counterstained with Hoechst 33258 (blue). Insets show boxed region at higher magnification.

(L, O, and P) Percentage of βIII tubulin-positive neurons (L), GFAP-positive astrocytes (O), or A2B5-positive oligodendrocyte precursors (P) in single-embryo cultures as in (K), (M), and (N), respectively (n ≥ 5 single embryos each).

*p < 0.05, ***p < 0.001. Scale bars, 13 (D), 100 (K), or 50 (M and N) μm (see also Figure S1). Error bars denote SEM.

and 2E). We then investigated gliogenesis, treating cultures for 5 days with either CNTF, which induces astrogenesis (Bonni et al., 1997), or neuregulin β, which enhances oligodendrogenesis (Canoll et al., 1996). Cultures were immunostained for CD44 or GFAP, markers of astrocyte precursors and later astrocytes, respectively, or for A2B5 and O4, markers of oligodendrocyte precursors and oligodendrocytes, respectively. Quantification showed that CBP knockdown decreased the genesis of both astrocytes (Figures 2D, 2F, and 2G) and oligodendrocytes (Figures 2D and 2H; see Figure 5G for A2B5).

To confirm these findings and to determine their relevance for RTS, we performed single-embryo cultures with progeny of $cbp^{+/-}$ crosses, ensuring similar cell densities for all genotypes (Figure S1C). Immunostaining at 2 days for Ki67, and counterstaining with Hoechst 33258 to reveal nuclear morphology, demonstrated that proliferation and survival were similar for $cbp^{+/+}$ and $cbp^{+/-}$ cortical precursors (Figures 2I and 2J and Figure S1C). In contrast, $cbp^{+/-}$ precursors generated fewer βIII-tubulin neurons at 3 days (Figures 2K and 2L), and fewer GFAP-positive astrocytes and A2B5-positive oligodendrocyte precursors after 5 days in CNTF or neuregulin β (Figures 2M–2P). Thus, CBP globally promotes cortical precursor differentiation, and *cbp* haploinsufficiency perturbs this function.

CBP Is Essential for Differentiation of Neurons and Glial Cells in the Embryonic Cortex

To determine if CBP also regulated cortical precursor differentiation in vivo, we performed in utero electroporations at E13/14 with *cbp* siRNAs and a nuclear EGFP expression plasmid (Barnabé-Heider et al., 2005; Bartkowska et al., 2007). When performed at this age, almost all electroporated cells are proliferating precursors that generate neurons embryonically and glia postnatally. Immunostaining 4 days postelectroporation confirmed the efficacy of the CBP knockdown, with *cbp* siRNAs

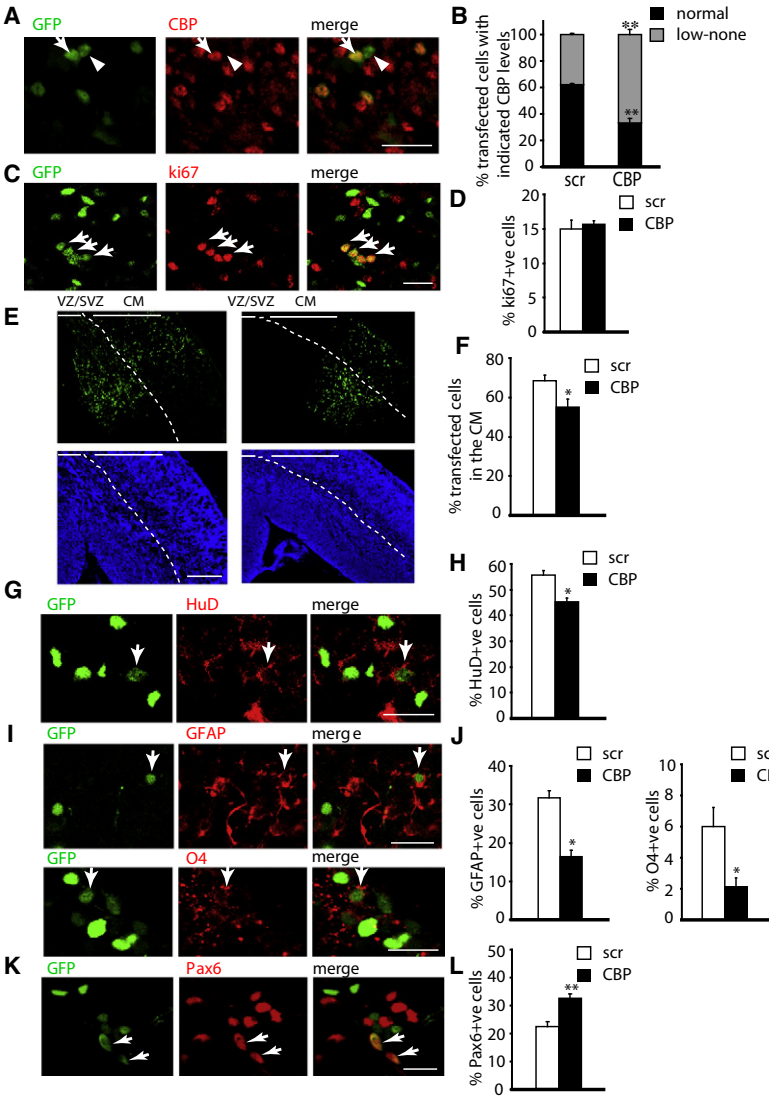

Figure 3. Genetic Knockdown of *cbp* Inhibits Neurogenesis and Gliogenesis In Vivo

(A) Confocal image of the VZ/SVZ electroporated with *cbp* siRNAs and immunostained for EGFP (green) and CBP (red). The arrow and arrowhead denote transfected cells expressing basal or no detectable CBP, respectively.

(B) Quantification of CBP immunoreactivity as in (A) for cells electroporated with scrambled versus *cbp* siRNAs.

(C) Confocal image of the VZ/SVZ electroporated with scrambled siRNA and doubled-labeled for EGFP (green) and Ki67 (red). Arrows denote double-labeled cells.

(D) Percentage of transfected, Ki67-positive cells in the VZ/SVZ as in (C) (n = ≥6 brains each).

(E) Immunocytochemistry for EGFP (green; Hoechst 33258 counterstain is blue) in coronal cortical sections electroporated with scrambled (left panels) or CBP (right panels) siRNAs. Dotted lines denote the VZ/SVZ and cortical mantle boundary.

(F) Percentage of EGFP-positive cells within the cortical mantle as in (E). n = at least 9 brains each.

(G) Confocal image of the cortical plate electroporated with *cbp* siRNA and double labeled for EGFP (green) and HuD (red). Arrows denote a double-labeled cell.

(H) Percentage of total transfected, HuD-positive cells in cortices as in (G) (n ≥ 5 brains each).

(I) Confocal images of the VZ/SVZ electroporated with scrambled siRNAs and double-labeled for EGFP (green) and GFAP (top) or O4 (bottom; both red) at P3. Arrows denote double-labeled cells.

(J) Percentage of transfected, GFAP-positive (left), or O4-positive (right) cells in the VZ/SVZ as in (I) (n ≥ 5 brains each).

(K) Confocal image of the VZ/SVZ electroporated with *cbp* siRNAs and doubled labeled for EGFP (green) and Pax6 (red) at E17/18. Arrows denote double-labeled cells.

(L) Percentage of transfected, Pax6-positive cells as in (K) (n ≥ 5 brains each).

E13/14 cortices were electroporated with *egfp* and *cbp* or scrambled siRNAs and analyzed at E16/17 (C and D), E17/18 (A, B, E–H, K, and L) or P3 (I and J). *p < 0.05, **p < 0.01. Scale bar, 20 (A, C, G, I, and K) or 250 μm (E). Error bars denote SEM.

increasing the percentage of transfected cells expressing little or no CBP protein (Figures 3A and 3B). CBP knockdown did not affect cortical precursor survival; at 3 days, only 2–5 *cbp* or scrambled siRNA-transfected cells per section expressed cleaved caspase-3 (data not shown). Similarly, CBP knockdown did not affect precursor proliferation, as indicated by immunostaining for Ki67 at 3 days (Figures 3C and 3D). In contrast, analysis of electroporated cortices at 4 days demonstrated an effect on neurogenesis. CBP knockdown decreased both the percentage of transfected cells that were in the cortical mantle, the region containing newborn neurons (Figures 3E and 3F), and the number that expressed the neuron-specific protein, HuD (Figures 3G and 3H). To investigate whether CBP was also important for gliogenesis in vivo, we performed our analyses at P3. Immunostaining for GFAP and O4 demonstrated that *cbp* siRNA-electroporated precursors generated many fewer astrocytes and oligodendrocytes (Figures 3I and 3J). Since CBP knockdown inhibits differentiation of neurons and glial cells, we immunostained for the radial precursor marker, Pax6, at 4 days to determine whether it coincidentally increased precursor numbers. Quantification indicated that this was indeed the case (Figures 3K and 3L).

To determine whether these perturbations persisted into adulthood, we analyzed $cbp^{+/-}$ versus $cbp^{+/+}$ cortices at P10, P50, and adulthood, focusing on the corpus callosum, since callosal abnormalities occur in RTS individuals. Measurement of corpus callosum thickness in Nissl-stained sections at the level of the rostral hippocampus (Bregma, −1.2 to −2.5; Figure 4A) demonstrated a 20% reduction in 75% of $cbp^{+/-}$ mice at P10 (Figure 4B), although this difference disappeared by P50 (Figure 4B). Densitometry of immunostained sections also showed that, at P10 and P50, 75% and 100%, respectively, of $cbp^{+/-}$ mice showed decreased GFAP immunoreactivity (Figures 4C and 4D). Consistent with this, chromatin immunoprecipitations (ChIP) and quantitative real-time PCR (qRT-PCR) demonstrated that CBP binding to and histone acetylation of the GFAP promoter and, to some degree, the MBP promoter, were decreased in P50 $cbp^{+/-}$ mice (Figure S2A). In contrast to these persistent

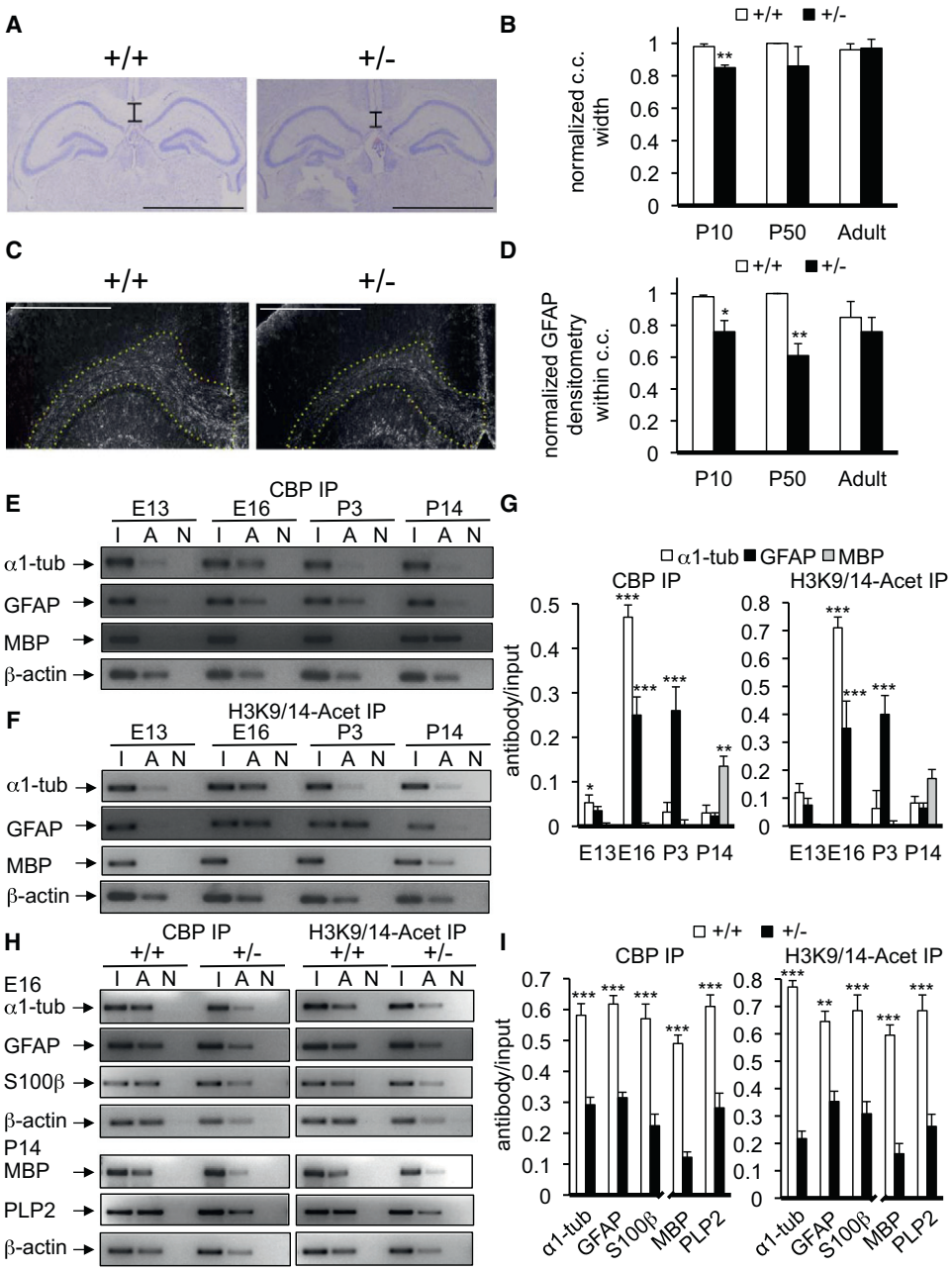

Figure 4. CBP Binds to and Acetylates Histones at Neural Promoters, and Regulates Corpus Callosum Development

(A–D) *cbp* haploinsufficiency causes deficits in the corpus callosum. (A) Nissl-stained sections of $cbp^{+/+}$ and $cbp^{+/-}$ P10 brains. Bars indicate the point at which corpus callosum thickness was measured. (B) Corpus callosum thickness as in (A) at P10, P50, and in adulthood (3 months to 1 year old); measurements were normalized to the controls ($n \geq 3$ brains each). (C) GFAP immunostaining in sections similar to those in (A). Hatched lines outline the corpus callosum. (D) Quantification by densitometry of GFAP immunoreactivity in the corpus callosum as in (C); measurements were normalized to controls. In (B) and (D), only the 75% of P10 $cbp^{+/-}$ brains that showed changes were included ($n \geq 3$ brains each).

(E–G) CBP binding to and histone acetylation of neural promoters during cortical development. ChIP analysis of *α1-tubulin*, *gfap*, *mbp*, and *β-actin* promoter regions for CBP binding (E and G) and for H3K9/14 acetylation (F and G) in E13, E16, P3, or P14 cortices. (E and F) Representative images of gels loaded with the amplified promoter regions from nonimmunoprecipitated input (I) or from immunoprecipitates with CBP or acetylated H3K9/14 antibodies (A), or with a control nonimmune IgG (N). (G) The qRT-PCR analysis (mean ± SEM) of the same samples (n = 3 animals/group; significance is relative to other promoters at the same time point).

(H and I) *cbp* haploinsufficiency causes decreased promoter binding and decreased histone acetylation during cortical development. ChIP analysis for CBP binding and H3K9/14 acetylation in E16 (α1-tubulin, GFAP, S100β promoters) or P14 (MBP, PLP2) $cbp^{+/+}$ versus $cbp^{+/-}$ cortices. (H) Representative images performed and labeled as in (E) and (F). (I) The qRT-PCR analysis of $cbp^{+/+}$ and $cbp^{+/-}$ cortices performed as in (G) (n = 3 animals/group).

*p < 0.05, **p < 0.01, ***p < 0.001. Scale bars, 2000 μm (A) and 1220 μm (C) (see also Figure S2). Error bars denote SEM.

perturbations in gliogenesis, no differences in the levels of olfactory bulb neurogenesis were observed in adult male *cbp*$^{+/-}$ versus *cbp*$^{+/+}$ mice (Figure S2B).

CBP Binds to Neuronal and Glial Gene Promoters and Globally Promotes Histone Acetylation in the Embryonic Cortex

To investigate whether CBP regulates differentiation by binding to and acetylating histones at promoters of neural differentiation genes, we performed ChIP assays. For neurons, we examined the α1-tubulin promoter, (Gloster et al., 1994), for oligodendrocytes, the myelin basic protein (MBP) promoter (Miura et al., 1989), and for astrocytes, the GFAP promoter (Miura et al., 1990). As a control, we used the β-actin promoter. Since CBP interacts with the general transcriptional apparatus, we focused upon the TATA box regions around these promoters (Figure S2C). Cross-linked DNA complexes, from cortices ranging in age from E13 to P14, were immunoprecipitated with antibodies specific for CBP or histone H3 acetylated at lysines 9 and 14 (H3K9/K14) (Weaver et al., 2004, 2005). Analysis of the uncross-linked, precipitated genomic DNA by semiquantitative and qRT-PCR demonstrated that CBP bound to all four promoters, with distinct time courses reflective of the genesis of the three different neural lineages (Figures 4E and 4G). For the neuronal α1-tubulin promoter, CBP was already bound at E13; binding peaked at E16, and then decreased postnatally, correlating with neurogenesis (Gloster et al., 1994). For GFAP, CBP binding peaked from E16 to P3, and decreased by P14, consistent with astrogenesis, while, for MBP, CBP was only bound postnatally, during the peak of oligodendrocyte maturation. In contrast, CBP bound the β-actin promoter at equal levels throughout cortical development (Figure 4E). Interestingly, in all cases, the relative pattern of H3K9/14 acetylation was similar to that of CBP binding (Figures 4F and 4G). Two-way ANOVA analysis of the qRT-PCR data revealed a highly significant gene × age interaction for the promoters with regard to both CBP ($F[2, 24] = 49.62$; $p = 0.0001$) and histone H3K9/K14 acetylation ($F[3, 23] = 60.32$; $p < 0.0001$).

To determine whether the level of histone acetylation at these promoters was a function of CBP binding, we isolated cortices from *cbp*$^{+/+}$ versus *cbp*$^{+/-}$ embryos, and performed ChIP analysis at E16 for α1-tubulin and GFAP, and at P14 for MBP. We also analyzed two additional glial promoters: S100β for astrocytes, and PLP2 for oligodendrocytes. These experiments showed decreased CBP binding and decreased H3K9/14 acetylation at all five promoters in CBP$^{+/-}$ cortices (Figures 4H and 4I). Statistical analyses of the qRT-PCR data indicated a main effect of genotype (*cbp*$^{+/+}$ versus *cbp*$^{+/-}$ mice: CBP IP, $[F(1, 17) = 334.2; p = 0.0001]$; acety-H3K9/14 IP, $[F(1, 17) = 124.3; p < 0.0001]$), while the interaction of gene with genotype was nonsignificant for both CBP ($F[2, 16] = 1.190$; $p > 0.05$) and H3K9/14 acetylation ($F[2, 16] = 1.078$; $p > 0.05$). Post hoc analysis indicated significant ($p < 0.001$) decreases in CBP binding and histone acetylation of all five promoters in *cbp*$^{+/-}$ versus *cbp*$^{+/+}$ cortices. Thus, *cbp* haploinsufficiency results in decreased histone acetylation of neural differentiation genes.

To determine whether the differentiation deficit seen when CBP was decreased was due to this decreased histone acetylation, we treated cortical precursors in which CBP was knocked down with the HDAC inhibitor, trichostatin A (TSA) (Yoshida and Horinouchi, 1999; Weaver et al., 2004, 2005) at a concentration (20–30 nM) that increased H3K9/K14 acetylation (Figure 5A), but did not affect survival. Quantification of transfected, βIII-tubulin-positive neurons at 5 days showed that TSA completely rescued the decreased neurogenesis seen with CBP

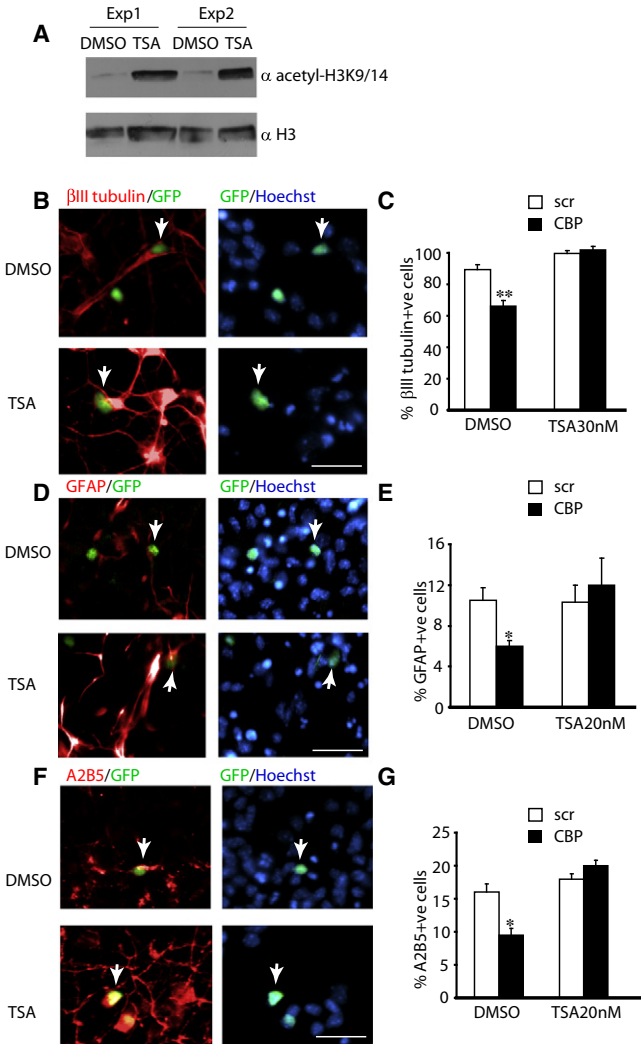

Figure 5. The HDAC Inhibitor, TSA, Rescues the Decreased Cortical Precursor Differentiation Caused by Genetic Knockdown of CBP

(A) Western blot for H3K9/14 acetylation in cortical precursors treated with DMSO or TSA in DMSO (20 nM) for 4 days. Blot was reprobed for total H3. Two of three similar experiments are shown (Exp1 and Exp2).

(B–G) Cortical precursors were cotransfected with *egfp* and *cbp* or scrambled (scr) siRNAs, and TSA at 30 nM (B and C) or 20 nM (D–G) was added 18 hr after transfection and 6–8 hr before adding CNTF (D and E) or neuregulin β (F and G) for 4 additional days. (B, D, and F) Immunocytochemistry for EGFP (green) and βIII-tubulin (B), GFAP (D), or A2B5 (F) (all red) in precursors transfected with scrambled siRNAs and cultured with DMSO alone (upper panels) or TSA in DMSO (lower panels). Cells were counterstained with Hoechst 33258 (blue). Arrows denote double-labeled, transfected cells. Scale bar, 25 μm. (C, E, and G) Quantification of the percentage of transfected, βIII tubulin-positive neurons (C), GFAP-positive astrocytes (E), or A2B5-positive oligodendrocyte precursors (G) in three experiments (pooled) similar to those in (B), (D), and (F), respectively. *$p < 0.05$, **$p < 0.01$. Error bars denote SEM.

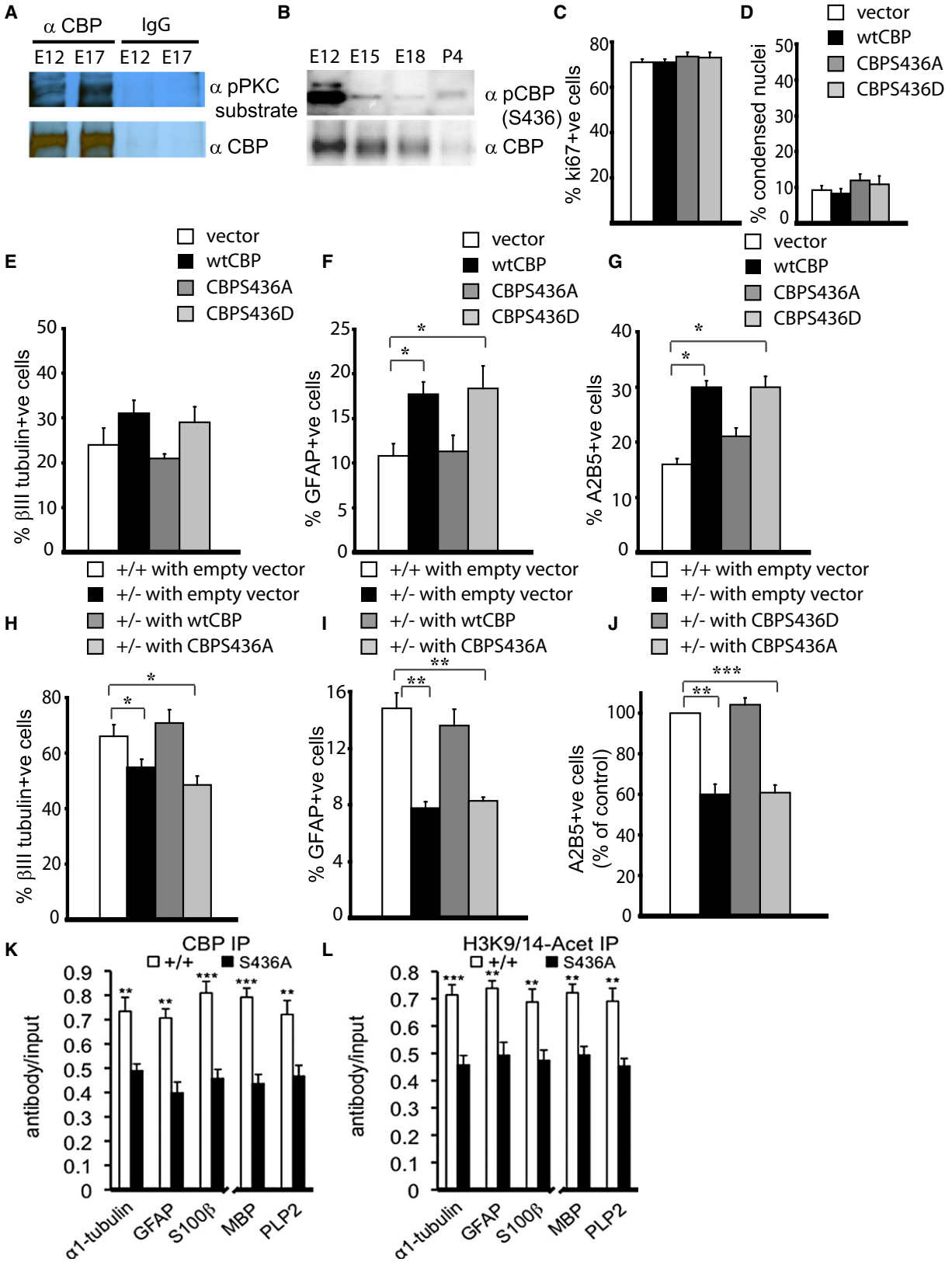

Figure 6. An aPKC Phosphorylation Site on CBP Is Essential for It to Promote Cortical Precursor Differentiation

(A) Western blot of E12 or E17 cortices immunoprecipitated with anti-CBP or control IgG, and probed with an antibody for phosphorylated PKC sites.

(B) Western blots of E12–P4 cortices probed with anti-phosphoS436 CBP and reprobed with anti-CBP.

knockdown (Figures 5B and 5C). A similar rescue of GFAP-positive astrocytes and A2B5-positive oligodendrocyte precursors was observed in CNTF or neuregulin β-treated cultures (Figures 5D–5G). Thus, CBP promotes precursor differentiation via histone acetylation.

CBP Requires Phosphorylation at an aPKC Site to Promote Neural Differentiation

To test the idea that the environment might enhance CBP activity to promote cortical precursor differentiation, we characterized a CBP serine 436 (S436) phosphorylation site that is downstream of a receptor tyrosine kinase-aPKC pathway in nonneural cells (He et al., 2009). CBP was immunoprecipitated from the E12–E17 cortex, and the immunoprecipitate was probed with an antibody that recognizes all phosphorylated PKC consensus sites (Figure 6A), or with a phospho-specific antibody for the S436 site (Figure 6B). This analysis showed that CBP was phosphorylated at PKC sites, including the S436 site, throughout embryonic cortical development.

To determine whether CBP S436 phosphorylation had any functional relevance for cortical precursors, we used plasmids encoding wild-type *cbp* or *cbp* mutants where S436 was mutated to an aspartate (*cbp*S436D), making it a phosphomimic, or to an alanine (*cbp*S436A), which cannot be phosphorylated (a phosphomutant) (Figure S3). Cortical precursors were transfected with these constructs and analyzed for survival and proliferation at 2 days, for neurogenesis at 3 days, and for gliogenesis following treatment with CNTF or neuregulin β for 5 days. None of these proteins affected cortical precursor survival or proliferation (Figures 6C and 6D). However, wild-type *cbp* and the *cbp* phosphomimic, but not the *cbp* phosphomutant, enhanced differentiation into astrocytes and oligodendrocytes (Figures 6F and 6G). A similar trend was observed for neurogenesis, but this did not reach significance (Figure 6E). We next performed similar experiments to determine whether these proteins could rescue the differentiation deficit seen with $cbp^{+/-}$ precursors. Expression of wild-type *cbp* or the *cbp* phosphomimic completely rescued the deficits in neurogenesis and gliogenesis seen in $CBP^{+/-}$ precursors (Figures 6H–6J), while the *cbp* phosphomutant had no effect (Figures 6H–6J). Thus, CBP must be phosphorylated at S436 to promote differentiation.

To investigate the relevance of these findings in vivo, we utilized mice in which the S436A phosphomutant CBP was knocked in to the CBP locus. These mice synthesize CBP at wild-type levels (Zhou et al., 2004). Through the use of ChIP assays, we determined cortical levels of CBP binding to and histone acetylation of neural promoters, analyzing the α1-tubulin, GFAP, and S100β promoters at birth, and the MBP and PLP2 promoters at P14. qRT-PCR demonstrated that CBP binding to and H3K9/K14 acetylation of these five promoters were decreased by almost half in $cbp^{S436A,S436A}$ cortices (Figures 6K and 6L). Statistical analyses of the qRT-PCR data indicated a main effect of genotype ($cbp^{+/+}$ versus $cbp^{S436A,S436A}$ mice: CBP IP, [$F(1, 17) = 421.3$; $p = 0.001$]; acety-H3K9/14 IP, [$F(1, 17) = 224.6$; $p < 0.001$]), while the interaction of gene with genotype was nonsignificant for both CBP ($F[2, 16] = 1.025$; $p > 0.05$) and histone H3K9/14 acetylation ($F[2, 16] = 1.014$; $p > 0.05$). Post hoc analysis indicated significant ($p < 0.01$) decreases in CBP binding and histone acetylation of all five promoters in $cbp^{S436A,S436A}$ versus $cbp^{+/+}$ cortices. Thus, CBP S436 phosphorylation directly regulates acetylation of histones on neural genes, thereby promoting neural precursor differentiation.

Atypical PKC-Mediated Phosphorylation Is Essential for CBP-Mediated Differentiation

To determine whether the kinase that phosphorylates the CBP S436 site to promote differentiation was aPKC, we first determined which aPKCs are expressed in cortical precursors. Western blots showed that aPKC ι and aPKC ζ II (also called aPKM ζ) were expressed in the embryonic cortex (Figure 7A). RT-PCR showed that *apkc* ζ I was also expressed in cultured cortical precursors and the embryonic cortex (Figure 7B). To determine if the CBP S436 site was downstream of aPKC, we cultured precursors with the general PKC inhibitor, chelerythrine chloride, a myristoylated peptide pseudosubstrate inhibitor of aPKCs ι/ζ, or an inhibitor of classical and novel PKCs, Gö6976. Western blots showed that chelerythrine chloride and the aPKC peptide inhibitor, but not Gö6976, decreased basal CBP S436 phosphorylation (Figure 7C). We next sought to learn whether inhibition of aPKC activity would inhibit the increased differentiation seen with CBP overexpression. Precursors were transfected with wild-type or phosphomimic CBP, and cultured for 5 days in CNTF or neuregulin β with one of the three PKC inhibitors. Chelerythrine chloride and the aPKC peptide inhibitor, but not Gö6976, completely blocked the CBP-mediated increase in astrocytes and oligodendrocytes (Figures 7D–7F). In contrast, they had no effect on differentiation promoted by phosphomimic CBP (Figures 7D–7F).

To confirm these results, we used a previously characterized shRNA for *apkc* ζ (He et al., 2009). Precursors were transfected with EGFP and *apkc* ζ shRNA and cultured for 3 days for neurogenesis and 5 days in CNTF or neuregulin β for gliogenesis. Immunostaining showed that aPKC ζ knockdown decreased the genesis of GFAP-positive astrocytes (Figure 7G) and A2B5-positive oligodendrocyte precursors (Figure 7H). The percentage of βIII-tubulin-positive neurons was also somewhat decreased, but this did not reach significance (Figure 7I). Consistent with

(C–G) Precursors were cotransfected with *egfp* and either wild-type *cbp* (wt *cbp*), phosphomutant *cbp* (*cbp* S436A), phosphomimic *cbp* (S436D), or empty vector for 2 (C and D), 3 (E), or 5 days in CNTF (F) or neuregulin β (G). Graphs show the percentage of transfected cells expressing Ki67(C), βIII tubulin (E), GFAP (F), A2B5 (G), or displaying apoptotic nuclei (D). In each case, three experiments were pooled.

(H–J) Single-embryo $cbp^{+/+}$ or $cbp^{+/-}$ precursor cultures were transfected with *egfp* and wt *cbp*, *cbp* S436D, *cbp* S436A, or the empty vector, and cultured for 3 days (H) or treated with CNTF (I) or neuregulin β (J) for 5 days. Graphs show percentage of transfected cells positive for βIII tubulin (H), GFAP (I), or A2B5 (J). In (J), results were normalized to wild-type cells with empty vector transfection (in all cases, $n \geq 3$ individual embryos, pooled).

(K and L) Quantification by ChIP assays and real-time PCR (mean ± SEM) of CBP binding (K) and H3K9/14 acetylation (L) in chromatin immunoprecipitated from $cbp^{+/+}$ or $cbp^{S436A,S436A}$ cortices at P1 (*α1-tubulin*, *GFAP*, and *S100β* promoters) or P14 (*mbp* and *plp2*) (n = 3 animals/group).

*$p < 0.05$, **$p < 0.01$, ***$p < 0.001$ (see also Figure S3). Error bars denote SEM.

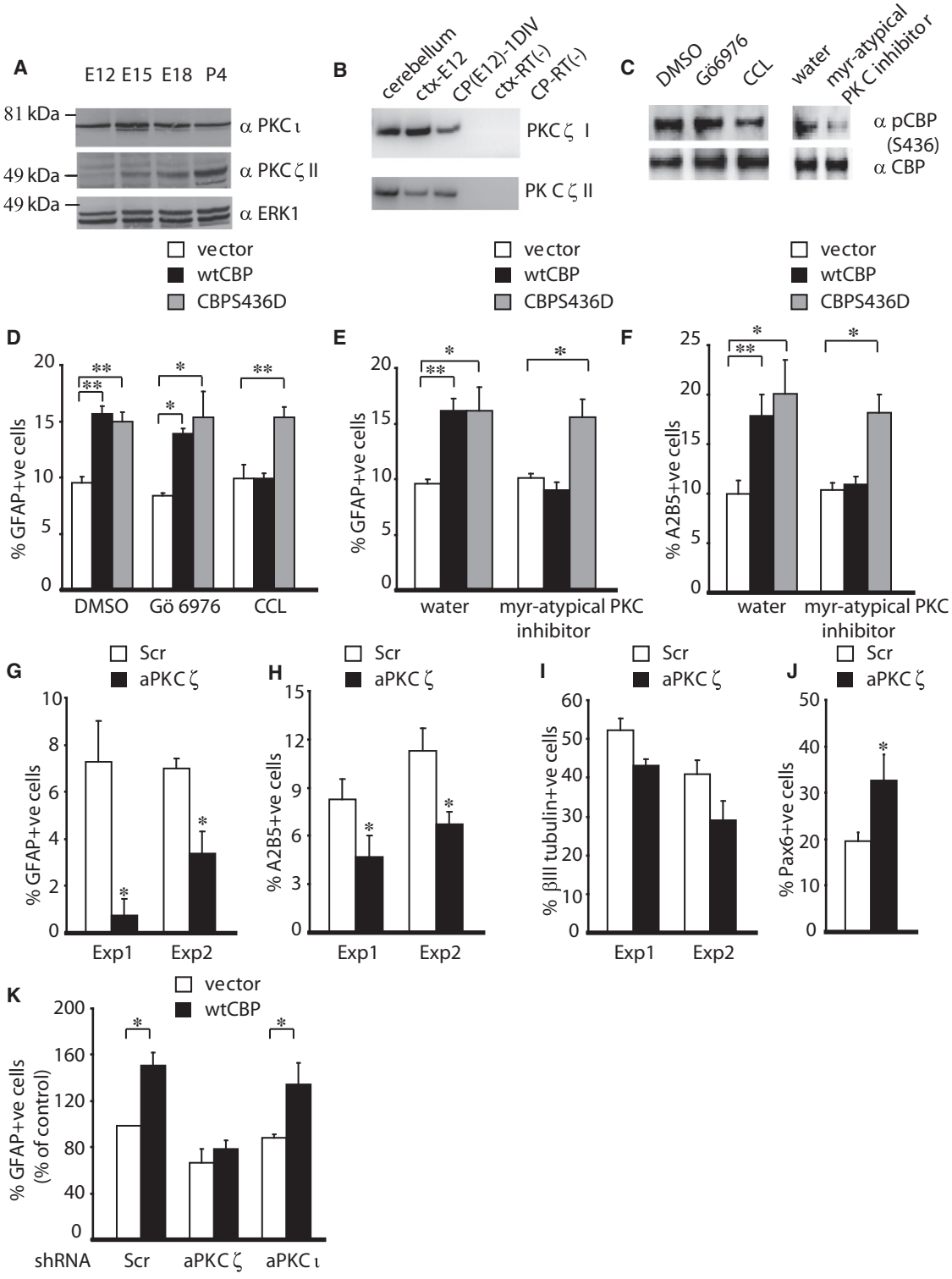

Figure 7. CBP Phosphorylation by aPKC Regulates Cortical Precursor Differentiation

(A) Western blots of E12–P4 cortical tissue for aPKC ι, aPKC ζ, and ERK (as a loading control).

(B) RT-PCR of E12 cortices (Ctx-E12) and E12 precursors cultured 1 day (CP(E12)-1DIV) for PKC ζ I and II. Cerebellar RNA was a positive control, and no reverse transcriptase was used (RT^-) as a negative control.

(C) Western blots for CBP S436 phosphorylation in precursors cultured in CNTF plus 250 nM Gö6976, 250 nM chelerythrine chloride (CCL), or 2 μM aPKC pseudosubstrate peptide inhibitor for 4 days commencing at 1 day. The blot was reprobed for CBP.

decreased differentiation, the percentage of Pax6-positive radial precursors was increased at 3 days (Figure 7J). Thus, aPKC ζ promotes cortical precursor differentiation.

We next investigated whether aPKC ζ was upstream of CBP during cortical precursor differentiation, as indicated by the pseudosubstrate inhibitor experiments (Figures 7E and 7F), focusing on astrogenesis. Precursors were cotransfected with wild-type CBP plus scrambled, *apkc* ζ, or *apkc* ι shRNAs, and cultured in the presence of CNTF for 5 days. Immunostaining for GFAP demonstrated that knockdown of aPKC ζ, but not aPKC ι, completely rescued the enhanced astrogenesis caused by CBP overexpression. Thus, aPKC ζ phosphorylates CBP to promote cortical precursor differentiation.

DISCUSSION

The data presented here support four major conclusions. First, the vocalization experiments indicate that, as seen in humans, *cbp* haploinsufficiency causes early cognitive deficits in mice. Some of these deficiencies persist, suggesting that the cognitive deficits documented in adult mice are at least partially due to abnormal development. Second, our studies with genetic knockdown or haploinsufficiency for *cbp* indicate that it is required for normal differentiation of cortical precursors in culture and in vivo; by binding sequentially to the promoters of neuronal, astrocytic, and oligodendroglial genes, CBP plays a crucial role in promoting differentiation into these three neural lineages. Moreover, CBP binding correlates with histone acetylation at these genes, and decreased CBP levels cause decreased histone acetylation. Third, we show that CBP HAT activity is required for cortical precursor differentiation, since the CBP knockdown phenotype can be rescued by coincident inhibition of HDACs. Fourth, we show that phosphorylation by aPKC ζ is essential for CBP to bind to neural promoters, to acetylate histones at those promoters, and to thereby trigger cortical precursor differentiation.

Based on these data, we propose a model where environmental signals activate aPKC ζ to phosphorylate CBP S436, thereby making cortical precursors competent to differentiate. One way in which CBP phosphorylation might do this is by directly regulating its HAT activity. A second possibility is that CBP phosphorylation modulates its interactions with transcriptional regulators, such as occurs in hepatocytes, where phosphorylation regulates CBPs interactions with CREB (He et al., 2009). Potential positive regulators include CBP-interacting proteins such as neurogenin (Sun et al., 2001), C/EBP (Kovacs et al., 2003), the STATs (Nakashima et al., 1999), or the olig bHLH transcription factors (Fukuda et al., 2004), all of which regulate cortical precursor differentiation (Miller and Gauthier-Fisher et al., 2007), while negative regulators include the CtBP corepressors, which bind CBP and regulate neural development (Senyuk et al., 2005). Regardless of mechanism, our model predicts that a decrease in phosphorylated CBP, as would occur in RTS or, potentially, even with some environmental perturbations, would lead to decreased neural cell genesis.

The model presented here provides one way to explain developmental changes in cortical precursor competence. In the early cortical neuroepithelium, precursors respond poorly to astrogenic cues, such as CT-1, and only become fully competent during the neurogenic period (Miller and Gauthier, 2007). While this change in competence is necessary to ensure that the precursor cell pool expands sufficiently, and that gliogenesis does not occur prematurely, the underlying mechanisms are still unclear. Histone methylation (Jepsen et al., 2007) and the ATP-dependent chromatin remodeling factor, Brg-1 (Seo et al., 2005), have been implicated, and our findings provide an additional mechanism where environmentally driven CBP phosphorylation could determine when a precursor can respond to gliogenic cues. What are the environmental cues that might regulate CBP S436 phosphorylation? We show here that aPKCs are the relevant upstream kinases, and previous work has shown that aPKC-mediated CBP S436 phosphorylation is downstream of an insulin-phosphatidylinositol 3-kinase (PI3K) pathway in hepatocytes (He et al., 2009). Interestingly, a number of growth factor receptors that activate PI3K and/or aPKC are important for cortical precursor differentiation, including the Trk neurotrophin receptors (Bartkowska et al., 2007), FGFR1 (Song and Ghosh, 2004), and erbB neuregulin receptors (Canoll et al., 1996).

These studies explain the early cognitive deficits seen in human RTS patients, where about 50% of patients carry a mutant *cbp* allele (Roelfsema and Peters, 2007). Several RTS mouse models have been generated in this regard, and all of them display deficits in adult learning and memory (Josselyn, 2005). While CBP is clearly important for adult neural circuits (Korzus et al., 2004), it is also important for neural development, since RTS individuals show early cognitive dysfunction (Roelfsema and Peters, 2007) and display neural dysgenesis, including cortical abnormalities and diminished white matter (Sener, 1995). We show here that $cbp^{+/-}$ mice also display early cognitive abnormalities and corpus callosum perturbations, arguing that the underlying molecular mechanisms may be similar in mice and humans.

Together, these findings provide a mechanism whereby environmental cues, acting via atypical PKC and CBP, can regulate stem cell epigenetic status and thereby directly promote differentiation. While we have studied cortical precursors here, this mechanism may well generalize to other developing or adult stem cell populations. Elucidating the environmental signals that regulate CBP activity, and thus histone acetylation and stem cell competence, will be an important direction for the future.

(D–F) Percentage of transfected, GFAP-positive astrocytes (D and E) or A2B5-positive oligodendrocyte precursors (F) in precursors cotransfected with *egfp* and wt *cbp*, *cbp* S436D, or empty vector, and cultured for 5 days in CNTF (D and E) or neuregulin β (F) plus 100 nM Gö6976, 100 nM chelerythrine chloride (D), or 1 μM aPKC pseudosubstrate inhibitor (E and F). In each case, four experiments were pooled.
(G–J) Percentage of transfected, GFAP-positive astrocytes (G), A2B5-positive oligodendrocyte precursors (H), βIII-tubulin-positive neurons (I), or pax6-positive radial precursors (J) in cultures cotransfected with *egfp* and scrambled, or aPKC ζ shRNA for 3 days (I and J) or 5 days in CNTF (G) or neuregulin β (H). In (G)–(I), Exp1 and Exp2 refer to two independent experiments. In (J), results from three experiments were pooled.
(K) Percentage of transfected, GFAP-positive astrocytes in precursors cotransfected with *egfp* and wild-type *cbp* or empty vector plus scrambled, *apkc* ζ, or *apkc* ι shRNAs and cultured for 5 days in CNTF. Results of three experiments were pooled.
*$p < 0.05$, **$p < 0.01$. Error bars denote SEM.

EXPERIMENTAL PROCEDURES

Animals

All animal use was approved by the Animal Care Committee for the Hospital for Sick Children in accordance with the Canadian Council of Animal Care policies. CD1 mice were obtained from Charles River Laboratory, and B6.126S6-*Crebbp*^{tm1Dli} mice from The Jackson Laboratory (Kung et al., 2000), and maintained in the same genetic background. *cbp* S436A knockin mice were maintained, bred, and genotyped as previously reported (He et al., 2009). For olfactory neurogenesis experiments, male *cbp*$^{+/+}$ and *cbp*$^{+/-}$ adult littermates were injected with 5 × 50 mg/ml BrdU at 3 hr intervals, and killed four weeks later (Kippin et al., 2005).

Cortical Precursor Cell Cultures

CD1 E11.5–E12.5 cortical precursors were cultured as described previously (Barnabé-Heider et al., 2005; Gauthier-Fisher et al., 2007). Plating density was 160,000 cells/ml for single-embryo cultures and plasmid transfections, and 285,000 cells/ml for siRNA transfections. For gliogenesis experiments, CNTF or neuregulin β were added 1 day after plating for an additional 4 days.

Transfections, Growth Factors, and Inhibitor Treatments

For siRNAs, precursors were transfected with 80 pmol *cbp* ON-TARGET plus SMARTpool siRNAs (proprietary mixture, Dharmacon) or a non-target scrambled siRNA pool. siRNAs were mixed with 1 μg of an EF-1α:EGFP plasmid (pEF-GM) plus 2 μl lipofectamine 2000 in 100 μl Opti-MEM (both from Invitrogen), incubated for 45 min, and added to precursors 2 hr after plating. For plasmids, 1 μg DNA (1:2 ratio of *egfp* versus *cbp* plasmids; 1:1:3 ratio of *egfp*, *apkc* shRNA, and *cbp* plasmids) and 1.5 μl Fugene 6 (Roche) were mixed with 100 μl Opti-MEM, incubated for 60 min, and added to precursors 2 hr after plating. The mouse *cbp* constructs and *apkc* shRNAs were as previously described (Zhou et al., 2004; He et al., 2009). NIH 3T3 cells and HEK293 cells were transfected with lipofectamine 2000. CNTF (50 ng/ml; Cedarlane Laboratories) and neuregulin β (100 ng/ml; R&D Systems) were added at 24–26 hr. Cells were treated with 20–30 nM TSA (Calbiochem) or 100–250 nM Gö6976 (Calbiochem), chelerythrine chloride (CCL; Calbiochem), or myristoylated aPKC pseudosubstrate peptide inhibitor (Calbiochem) were added 18 hr after transfection and 6–8 hr before adding growth factors.

RT-PCR

cDNA was synthesized from total RNA with the SuperScript Preamplification System cDNA Synthesis Kit (Invitrogen). Primers and conditions are in Supplemental Experimental Procedures.

In Utero Electroporation

In utero electroporation was performed as previously described (Barnabé-Heider et al., 2005; Gauthier-Fisher et al., 2009) with E13/E14 CD1 mice, injecting 4 μg pEF-*egfp*, 20 pmol siRNAs, and 0.05% Trypan blue.

Immunocytochemistry and Histological Analysis

Immunocytochemistry and Nissl staining were performed as previously described (Gauthier-Fisher et al., 2007). For BrdU/NeuN colocalization, sections were incubated in 1 N HCl at 60°C after fixation and before blocking, and sequential immunocytochemistry was performed. Antibodies are in Supplemental Experimental Procedures.

Microscopy, Confocal Analysis, and Quantification

For precursor cultures, approximately 200 cells per condition in at least 8 randomly chosen fields per experiment were counted. Digital image acquisition was performed with Northern Eclipse software (Empix) with a Sony XC-75CE CCD video camera. For in utero electroporation, three to four fields per coronal section from each of five anatomically matched sections per brain were analyzed on a Zeiss Pascal confocal microscope with the manufacturer's software. A mean of four scans taken with a 40× objective were computed for each image. For postnatal mice, all studies were blinded, analyzing three to five coronal sections encompassing the rostral hippocampus per brain (Bregma, −1.2 to −2.5). ImageJ software (NIH) was used to measure corpus callosum thickness from digital images of Nissl-stained sections acquired with a Mirax slide scanner, or as described above. For GFAP densitometry, three to four images of each hemisphere (total six to eight images) were acquired per brain. The corpus callosum was defined by Hoechst staining, and the GFAP signal thresholded and measured with Northern Eclipse software. For quantification of adult olfactory neurogenesis, serial coronal olfactory bulb sections were immunostained for BrdU and NeuN, and double-labeled cells were counted in every 20th section. Statistical analyses were performed with Student's t test. In all cases, error bars indicate SEM.

Western Blot Analysis and Immunoprecipitations

Cells and tissues were lysed in RIPA lysis buffer, 50-100 μg protein lysate run on SDS-PAGE, and Western blots performed as previously described (Barnabé-Heider et al., 2005). For immunoprecipitation, equal amounts of protein from embryonic cortical lysates were incubated with 15 μl of the CBP antibody (Santa Cruz Biotechnology) for 1 hr at 4°C and then incubated for the same time period with 30 μl protein A-Sepharose (Sigma). Precipitated proteins were collected by centrifugation, washed three times with RIPA lysis buffer, boiled with sample buffer, and loaded on a 7.5% SDS-PAGE gel.

ChIP Assay

ChIP assays were performed as previously described (Weaver et al., 2004, 2005). Embryonic and neonatal cortices were dissected in ice-cold HBSS buffer, and the chromatin was cross-linked with 1% formaldehyde, sheared down by sonication, and immunoprecipitated with one of the following: rabbit polyclonal anti-acetyl-histone H3K9/K14 (Cell Signaling Technology), rabbit polyclonal anti-CBP (Santa-Cruz Biotechnology), or rabbit nonimmune IgG antibody (Santa Cruz Biotechnology). One-tenth of the lysate was kept to quantify DNA before immunoprecipitation ("input"). Protein-DNA complexes were un-cross-linked and DNA extracted, precipitated, and resuspended in 1× TE (100 μl). The mouse *α1-tubulin* (MGI 98869), *gfap* (MGI 95697), *S100β* (MGI 98217), *mbp* (MGI 96925), *plp2* (MGI 1298382), or *β-actin* (MGI 87904) TATA box promoter regions of the un-cross-linked DNA was subjected to real-time qRT-PCR amplification, with primers described in the Supplemental Experimental Procedures. PCR reactions were done with the FailSafe GREEN Real-Time PCR Pre-Mix-Choice Kit protocol (Epicenter; InterScience, Canada), as described in Supplemental Experimental Procedures, with a LightCycler 480 (Roche Molecular Biochemicals). All reactions were performed in triplicate, and a no-template negative control was included for each set of primers. No primer-dimers were detected. To calculate fold change in gene expression, the ratio of the immunoprecipitate/input mean crossing-point values were determined for each promoter and, where possible, divided by the same ratio for the β-actin promoter-α region amplified from the same precipitate. Amplified products were also separated on agarose gels (2%), and bands were captured with the image acquisition software, Gene Snap (Synoptics Ltd., USA) on a Syngene Bio Imaging System (Synoptics Ltd., USA).

Ultravocalization Test

P10 *cbp*$^{+/+}$ and *cbp*$^{+/-}$ mice were assessed for USV with an Ultrasound Detector D 1000X (Pettersson Elektronik AB, Uppsala, Sweden) as previously described (Wang et al., 2008; Supplemental Experimental Procedures). All testing was carried out under dim red light in a quiet room. Statistical analyses were performed with two-tailed Student's t tests.

SUPPLEMENTAL INFORMATION

Supplemental Information includes three figures and Supplemental Experimental Procedures and can be found with this article online at doi:10.1016/j.devcel.2009.10.023.

ACKNOWLEDGMENTS

This work was supported by Canadian Institutes of Health Research (CIHR) grant MOP13958 to F.D.M. and D.R.K. F.D.M. and D.R.K. are Canada Research Chairs, and F.D.M. is a Howard Hughes Medical Institute International Research Scholar. J.W. and I.C.G.W. were supported by fellowships from the Hospital for Sick Children Foundation/Multiple Sclerosis Society of

Canada, and the CIHR, respectively. We thank Bill Trimble, Dennis Aquino, and Kaplan/Miller laboratory members for advice and assistance.

Received: February 17, 2009
Revised: August 10, 2009
Accepted: October 27, 2009
Published: January 19, 2010

REFERENCES

Barnabé-Heider, F., Wasylnka, J.A., Fernandes, K.J., Porsche, C., Sendtner, M., Kaplan, D.R., and Miller, F.D. (2005). Evidence that embryonic neurons regulate the onset of cortical gliogenesis via cardiotrophin-1. Neuron *48*, 253–265.

Bartkowska, K., Paquin, A., Gauthier, A.S., Kaplan, D.R., and Miller, F.D. (2007). Trk signaling regulates neural precursor cell proliferation and differentiation during cortical development. Development *134*, 4369–4380.

Bonni, A., Sun, Y., Nadal-Vicens, M., Bhatt, A., Frank, D.A., Rozovsky, I., Stahl, N., and Yancopoulos, G.D. (1997). Regulation of gliogenesis in the central nervous system by the JAK-STAT signaling pathway. Science *278*, 477–483.

Branchi, I., Santucci, D., and Alleva, E. (2001). Ultrasonic vocalization emitted by infant rodents: a tool for assessment of neurobehavioral development. Behav. Brain Res. *125*, 49–56.

Canoll, P.D., Musacchio, J.M., Hardy, R., Reynolds, R., Marchionni, M.A., and Salzer, J.L. (1996). GGF/neuregulin is a neuronal signal that promotes the proliferation and survival and inhibits the differentiation of oligodendrocyte progenitors. Neuron *17*, 229–243.

Chan, H.M., and La Thangue, N.B. (2001). p300/CBP proteins: HATs for transcriptional bridges and scaffolds. J. Cell Sci. *114*, 2363–2373.

Fukuda, S., Kondo, T., Takebayashi, H., and Taga, T. (2004). Negative regulatory effect of an oligodendrocytic bHLH factor OLIG2 on the astrocytic differentiation pathway. Cell Death Differ. *11*, 196–202.

Gauthier-Fisher, A., Furstoss, O., Araki, T., Chan, R., Neel, B.G., Kaplan, D.R., and Miller, F.D. (2007). Control of CNS cell-fate decisions by SHP-2 and its dysregulation in Noonan syndrome. Neuron *54*, 245–262.

Gauthier-Fisher, A.S., Lin, D., Greeve, M., Kaplan, D.R., Rottapel, R., and Miller, F.D. (2009). Lfc and Tctex-1 regulate the genesis of neurons from cortical radial precursors. Nat. Neurosci. *12*, 735–744.

Gloster, A., Wu, W., Speelman, A., Weiss, S., Causing, C., Pozniak, C., Reynolds, B., Chang, E., Toma, J.G., and Miller, F.D. (1994). The tα1 α-tubulin promoter specifies gene expression as a function of neuronal growth and regeneration in transgenic mice. J. Neurosci. *14*, 7319–7330.

Haberland, M., Montgomery, R.L., and Olson, E.N. (2009). The many roles of histone deacetylases in development and physiology: implications for disease and therapy. Nat. Rev. Genet. *10*, 32–42.

He, L., Sabet, A., Djedjos, S., Miller, R., Sun, X., Hussain, M.A., Radovick, S., and Wondisford, F.E. (2009). Metformin and insulin suppress hepatic gluconeogenesis by inhibiting cAMP signaling through phosphorylation of CREB binding protein (CBP). Cell *137*, 635–646.

Jepsen, K., Solum, D., Zhou, T., McEvilly, R.J., Kim, H.J., Glass, C.K., Hermanson, O., and Rosenfeld, M.G. (2007). SMRT-mediated repression of an H3K27 demethylase in progression from neural stem cell to neuron. Nature *450*, 415–419.

Josselyn, S.A. (2005). What's right with my mouse model? New insights into the molecular and cellular basis of cognition from mouse models of Rubinstein-Taybi syndrome. Learn. Mem. *12*, 80–83.

Kippin, T.E., Martens, D.J., and van der Kooy, D. (2005). p21 loss compromises the relative quiescence of forebrain stem cell proliferation leading to exhaustion of their proliferation capacity. Genes Dev. *19*, 756–767.

Korzus, E., Rosenfeld, M.G., and Mayford, M. (2004). CBP histone acetyltransferase activity is a critical component of memory consolidation. Neuron *42*, 961–972.

Kovacs, K.A., Steinmann, M., Magistretti, P.J., Halfon, O., and Cardinaux, J.R. (2003). CCAAT/enhancer-binding protein family members recruit the coactivator CREB-binding protein and trigger its phosphorylation. J. Biol. Chem. *278*, 36959–36965.

Kung, A.L., Rebel, V.I., Bronson, R.T., Chang, L.E., Sieff, C.A., Livingston, D.M., and Yao, T.P. (2000). Gene dose-dependent control of hematopoiesis and hematologic tumor suppression by CBP. Genes Dev. *14*, 272–277.

Lunyak, V.V., and Rosenfeld, M.G. (2008). Epigenetic regulation of stem cell fate. Hum. Mol. Genet. *17*, R28–R36.

Miller, F.D., and Gauthier, A.S. (2007). Timing is everything: making neurons versus glia in the developing cortex. Neuron *54*, 357–369.

Miura, M., Tamura, T., Aoyama, A., and Mikoshiba, K. (1989). The promoter elements of the mouse myelin basic protein gene function efficiently in NG108-15 neuronal/glial cells. Gene *75*, 31–38.

Miura, M., Tamura, T., and Mikoshiba, K. (1990). Cell-specific expression of the mouse glial fibrillary acidic protein gene: identification of the cis- and trans-acting promoter elements for astrocyte-specific expression. J. Neurochem. *55*, 1180–1188.

Nakashima, K., Yanagisawa, M., Arakawa, H., Kimura, N., Hisatsune, T., Kawabata, M., Miyazono, K., and Taga, T. (1999). Synergistic signaling in fetal brain by STAT3-Smad1 complex bridged by p300. Science *284*, 479–482.

Rebel, V.I., Kung, A.L., Tanner, E.A., Yang, H., Bronson, R.T., and Livingston, D.M. (2002). Distinct roles for CREB-binding protein and p300 in hematopoietic stem cell self-renewal. Proc. Natl. Acad. Sci. USA *99*, 14789–14794.

Roelfsema, J.H., and Peters, D.J. (2007). Rubinstein-Taybi syndrome: clinical and molecular overview. Expert Rev. Mol. Med. *9*, 1–16.

Sener, R.N. (1995). Rubinstein-Taybi syndrome: cranial MR imaging findings. Comput. Med. Imaging Graph. *19*, 417–418.

Senyuk, V., Sinha, K.K., and Nucifora, G. (2005). Corepressor CtBP1 interacts with and specifically inhibits CBP activity. Arch. Biochem. Biophys. *441*, 168–173.

Seo, S., Richardson, G.A., and Kroll, K.L. (2005). The SWI/SNF chromatin remodeling protein Brg1 is required for vertebrate neurogenesis and mediates transactivation of Ngn and NeuroD. Development *132*, 105–115.

Song, M.R., and Ghosh, A. (2004). FGF2-induced chromatin remodeling regulates CNTF-mediated gene expression and astrocyte differentiation. Nat. Neurosci. *7*, 229–235.

Sun, Y., Nadal-Vicens, M., Misono, S., Lin, M.Z., Zubiaga, A., Hua, X., Fan, G., and Greenberg, M.E. (2001). Neurogenin promotes neurogenesis and inhibits glial differentiation by independent mechanisms. Cell *104*, 365–376.

Wang, H., Liang, S., Burgdorf, J., Wess, J., and Yeomans, J. (2008). Ultrasonic vocalizations induced by sex and amphetamine in M2, M4, M5 muscarinic and D2 dopamine receptor knockout mice. PloS One *3*, e1893.

Weaver, I.C., Cervoni, N., Champagne, F.A., D'Alessio, F.A., Sharma, A.C., Seckl, S., Jr., Dymov, S., Szyf, M., and Meaney, M.J. (2004). Epigenetic programming by maternal behavior. Nat. Neurosci. *7*, 847–854.

Weaver, I.C., Champagne, F.A., Brown, S.E., Dymov, S., Sharma, S., Meaney, M.J., and Szyf, M. (2005). Reversal of maternal programming of stress responses in adult offspring through methyl supplementation: altering epigenetic marking later in life. J. Neurosci. *25*, 11045–11054.

Yoshida, M., and Horinouchi, S. (1999). Trichostatin and leptomycin. Inhibition of histone deacetylation and signal-dependent nuclear export. Ann. N Y Acad. Sci. *886*, 23–36.

Zhou, X.Y., Shibusawa, N., Naik, K., Porras, D., Temple, K., Ou, H., Kaihara, K., Roe, M.W., Brady, M.J., and Wondisford, F.E. (2004). Insulin regulation of hepatic gluconeogenesis through phosphorylation of CREB-binding protein. Nat. Med. *10*, 633–637.